# MATHEMATICAL MODELING OF THE ATTITUDE TRACKER

B.Gokhman and F. C. Billingsley
Jet Propulsion Laboratory,
California Institute of Technology
Pasadena, California 91109, USA.
Comission III.

## 1. Introduction

Future sensors of the linear array type will return lines of data which are independent in the sense that there is no data tie between them. It is essential for mapping and stereo work that the data lines used for analysis be in precisely the correct geometrical position. If the sensed image lines are not in the correct positions, interpolation or other compensation must be used before analysis. Position determination depends on the exact knowledge of the platform attidude. While the spacecraft control parameters will be marginally adequate, the problem is exacerbated with an aircraft platform due to the ubiquitous platform instability. The use of ground control points will be necessary for precise tie to the ground, but would be cumbersome for continued use for the altitude tracking, and in any event, surveyed ground control points will not be available for many areas. What is needed is a system, capable of analyzing the platform motion from the collected image information, which can be used to verify the platform stability and to provide the data for geometric correction. This may be used to further improve the expected good performance of the platform or to compensate for any degraded performance.

## 2. System design

The design concept of the attitude tracker system was proposed by F.C. Billingsley (Billingsley,1982). Consider a 3 X 3 array of small (relative to the length of the imaging line array) square imaging devices placed in the focal plane of the camera (Figure 1).

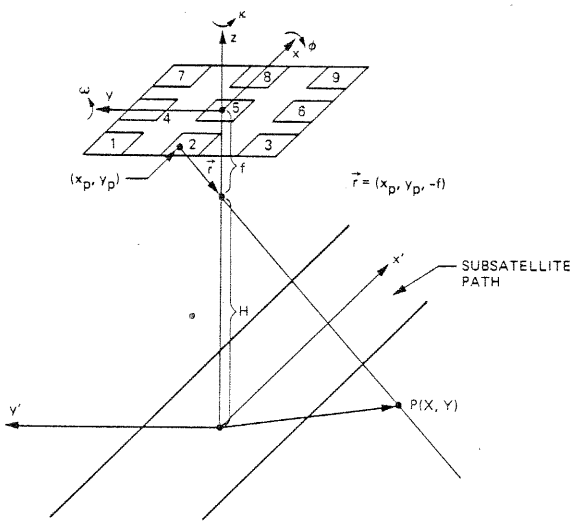


Figure 1. System geometry.

All nine images are read simultaneously into a set of memories. For each image the displacement between it and a prior corresponding image taken within a short time interval is calculated. The set of nine displacement vectors form the data for determining the change in attitude occuring between the two samplings. The time-sequential set of displacement vectors may be used to calculate the platform attitude variation history, and to generate the geometric correction parameters. Data analysis follows the well known stereo compilation principles. The effects as seen in normal stereo compilation practice are given in Figure 2 (from D. H. Alspaugh, 1979). Figure 2 shows the displacement vector components, resulting from translation in three dimensions and three Euler rotations (roll, pitch and yaw).

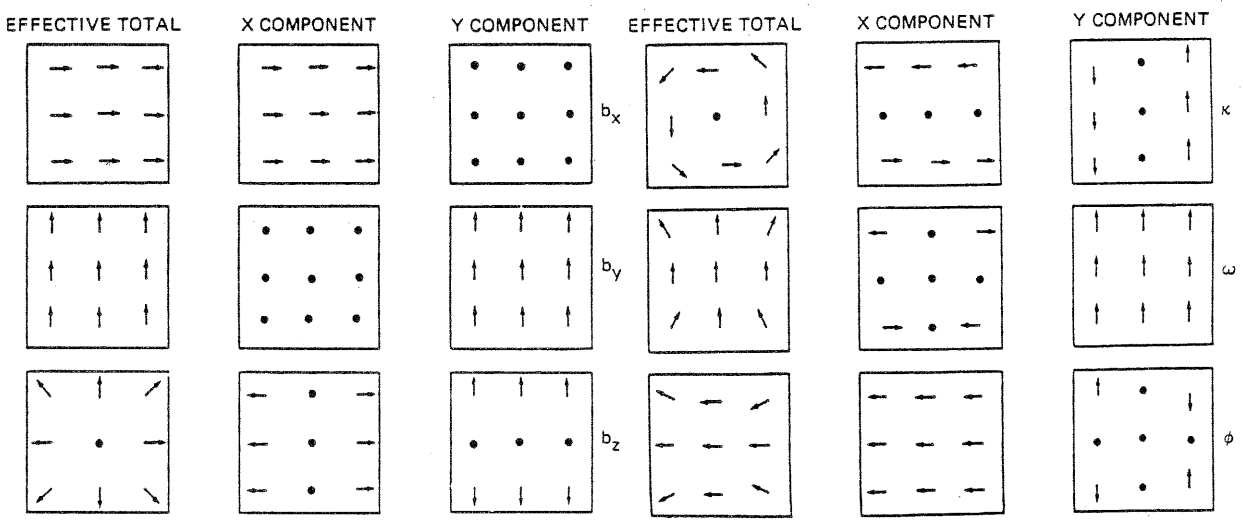


Figure 2. The image motion vector set.

## 3. Formulation

### 3.1 Geometry

Figure 1 shows the geometry of the problem. Nine square imaging devices (32 X 32, 64 X 64, etc. pixel CCD arrays) are placed in the focal plane of the instrument. We select the frame of reference (x,y,z) tied to the instrument so that the z-axis is perpendicular to the focal plane, pointing to the zenith, x-axis pointing in the direction of platform motion and y-axis forming the righthand system. The origin of this frame coincides with the center of the center array #5. We also select an inertial frame

$(x',y',z')$ such that the plane $(x',y')$ coincides with the ground plane, origin being in the nadir point. We restrict the derivation here to the flat Earth approximation, assuming that it can be easily generalized.

## 3.2 Lookpoint model

The attitude of the platform can be best described by the set of Euler angles: roll, pitch and yaw. The lookpoint, that is the point on the ground, imaged by a detector element (pixel), is the point of intersection of the light ray, emanating from the pixel and coming through the focal point, with the ground plane. For the nine arrays the vector, colinear with such a ray has components:

$$\mathbf{r}=(x_p,y_p,-f)^T$$

where:

$x_p$, $y_p$ define the pixel position;

$f$ is the focal length of the instrument.

The platform attitude in the ground reference frame after an arbitrary rotation is most easily defined by a set of Euler matrixes:

$$\mathbf{M}(\phi)=\begin{bmatrix}1 & 0 & 0\\ 0 & \cos(\phi) & \sin(\phi)\\ 0 & -\sin(\phi) & \cos(\phi)\end{bmatrix} \qquad \mathbf{M}(\omega)=\begin{bmatrix}\cos(\omega) & 0 & -\sin(\omega)\\ 0 & 1 & 0\\ \sin(\omega) & 0 & \cos(\omega)\end{bmatrix}$$

$$\mathbf{M}(\chi)=\begin{bmatrix}\cos(\chi) & \sin(\chi) & 0\\ -\sin(\chi) & \cos(\chi) & 0\\ 0 & 0 & 1\end{bmatrix} \tag{3.2.1}$$

where:

$\phi$ is roll angle;
$\omega$ is pitch angle;
$\chi$ is yaw angle.

The combination of three Euler rotations is determined by the matrix product $\mathbf{M}(\phi,\omega,\chi)=\mathbf{M}(\phi)\mathbf{M}(\omega)\mathbf{M}(\chi)$, so that the components of $\mathbf{r}$ in the ground reference frame are defined as:

$$\mathbf{r}'(x',y',z')=\mathbf{M}\mathbf{r}(x,y,z). \tag{3.2.2}$$

Now, from the similarity of the triangles, the ground coordinates of the lookpoint $P(X_G,Y_G)$ are easily obtained:

$$X_G = (x'/z')H; \tag{3.2.3}$$

$$Y_G = (y'/z')H;$$

where H is the altitude of the platform.

## 3.3 Attitude restoration

We thus obtained the ground position of the lookpoint P as a function of the Euler angles and altitude:

(3.3.1) $$P_{X,Y}=P(\mathbf{r}'(\phi,\omega,\chi),H)=P(\mathbf{M}(\phi,\omega,\chi)\mathbf{r},H).$$

Here vector $\mathbf{r}$ is only a function of the camera geometry, depending on the location of the pixel in the focal plane and on the focal length. The left part of equation (3.3.1) is obtained by measuring the components of the displacement vector, by comparing the time-sequential images for each detector array, as described before. Each detector array yields two equations, one for every vector component. Since the dependency of the vector components on altitude H is clearly linear, H can be omitted (set to 1), this corresponds to a simple scale change. In the particular case of nine arrays one obtaines the system of 18 equations, as follows:

(3.3.2)
$$\begin{aligned} X_1&=X(\mathbf{M}(\phi,\omega,\chi)\mathbf{r}_1);\\ Y_1&=Y(\mathbf{M}(\phi,\omega,\chi)\mathbf{r}_1);\\ &\vdots\\ X_9&=X(\mathbf{M}(\phi,\omega,\chi)\mathbf{r}_9);\\ Y_9&=Y(\mathbf{M}(\phi,\omega,\chi)\mathbf{r}_9). \end{aligned}$$

We can now resolve (3.3.2) with respect to $\phi$, $\omega$ and $\chi$. Since this system is overdetermined (the number of equations is greater than the number of unknowns) we apply the standard least-square fitting procedure. The solution is greatly simplified in the case of small angles, when the rotation matrix can be replaced by its linear approximation, as follows:

(3.3.3) $$\mathbf{M}(\phi,\omega,\chi)=\begin{bmatrix} 1 & \chi & -\omega \\ -\chi+\phi\omega & 1+\phi\omega\chi & \phi \\ -\phi\chi+\omega & -\phi+\omega\chi & 1 \end{bmatrix}$$

Formula (3.3.3) is obtained by multiplying matrixes $\mathbf{M}(\phi)$, $\mathbf{M}(\omega)$ and $\mathbf{M}(\chi)$ from (3.2.1) and replacing $\sin(\alpha)$ and $\cos(\alpha)$ by $\alpha$ and 1 respectively. Now equations (3.2.2) can be re-written as follows:

(3.3.4)
$$\begin{aligned} x'&=X_p+\chi Y_p-\omega Z_p;\\ y'&=(-\chi+\phi\omega)X_p+(1+\phi\omega\chi)Y_p+\phi Z_p\\ z'&=(-\phi\chi+\omega)X_p+(-\phi+\omega\chi)Y_p+Z_p \end{aligned}$$

and, substituting (3.3.4) into (3.2.3) and retaining only the first order terms with respect to $\phi$, $\omega$ and $\chi$ we finally obtain:

(3.3.5) $X_G=(x'/z')=[\ X/Z + \phi XY/Z^2 - \omega(1+X^2/Z^2) + \chi Y/Z\ ];$

$Y_G=(y'/z')=[\ Y/Z + \phi(1+Y^2/Z^2) - \omega XY/Z^2 - \chi X/Z\ ].$

## 3.4 Displacement vector extraction

The left part of (3.3.5) represents the components of the displacement vector, and must be determined as a result of the measurement.

To compute the displacement we use the phase correlation technique, described by Kuglin and Hines (Kuglin and Hines,1975). The phase correlation method uses the fact that the information pertaining to the displacement of two images resides in the phase of the cross power spectrum. The phase correlation function is obtained by first computing the discrete two-dimensional Fourier transforms, and extracting the phase of the cross-power spectrum of two images, $G_1$ and $G_2$:

$$e^{jf} = \frac{G_1 G_2^*}{|\ G_1 G_2^*\ |}$$

and then computing the inverse Fourier transform of the phase array

$$d = F^{-1}\{\ e^{jf}\ \}.$$

The last equation yields a sharp peak located at the position corresponding to the displacement vector.
This method is relatively scene-independent, exibits an extremely narrow correlation peak, and is insensitive to narrow bandwidth noise. However, in the digital implementation used, only integer pixel displacement are used, so that displacement to only the nearest pixel is available.

## 4. Simulation

### 4.1 Lookpoint model and image extraction

For the purpose of this simulation, the displacement vector components are determined from the comparison of the time-sequential subimages, extracted from a LANDSAT Thematic Mapper frame.
The square detector array not parallel to the ground will generally image a trapezoidal area. To extract the portion of the TM scene as "seen" by our nine arrays, we first compute the location of the corners and the centers of the nine array

projections onto the ground. The results of these computations are shown on Figure 3. Shown here are the outlines of the detector arrays, subjected to the simultaneous roll, pitch and yaw of +0.1, -0.1 and 0.0 radian.
Figure 4 shows the path on the ground traced by the nine detector arrays when the translation is applied simultaneously with the Euler rotations.

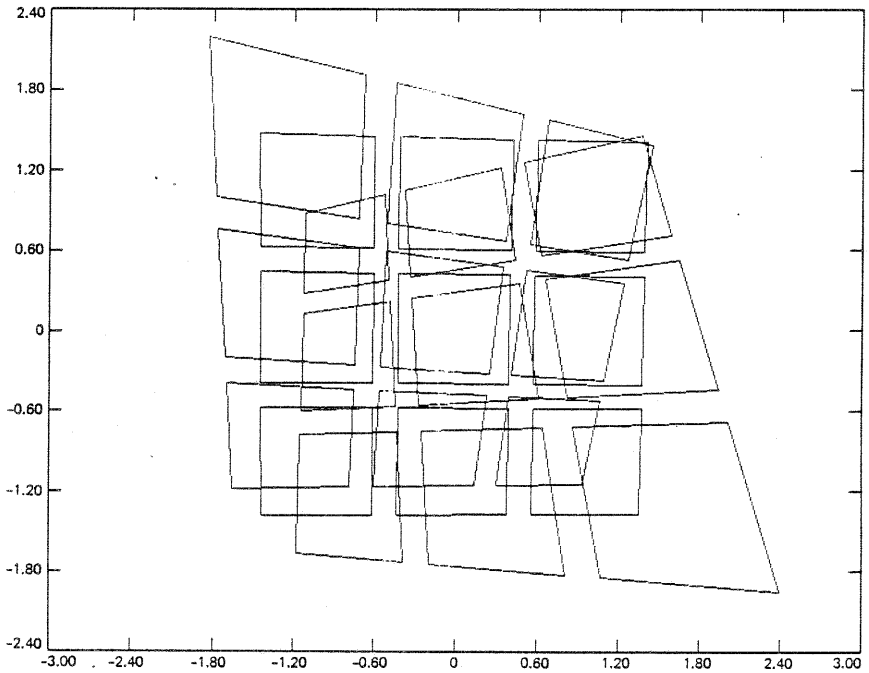


Figure 3. Projections of the nine arrays onto the ground at the roll, pitch and yaw values of ±0.1 and 0.0 radian.

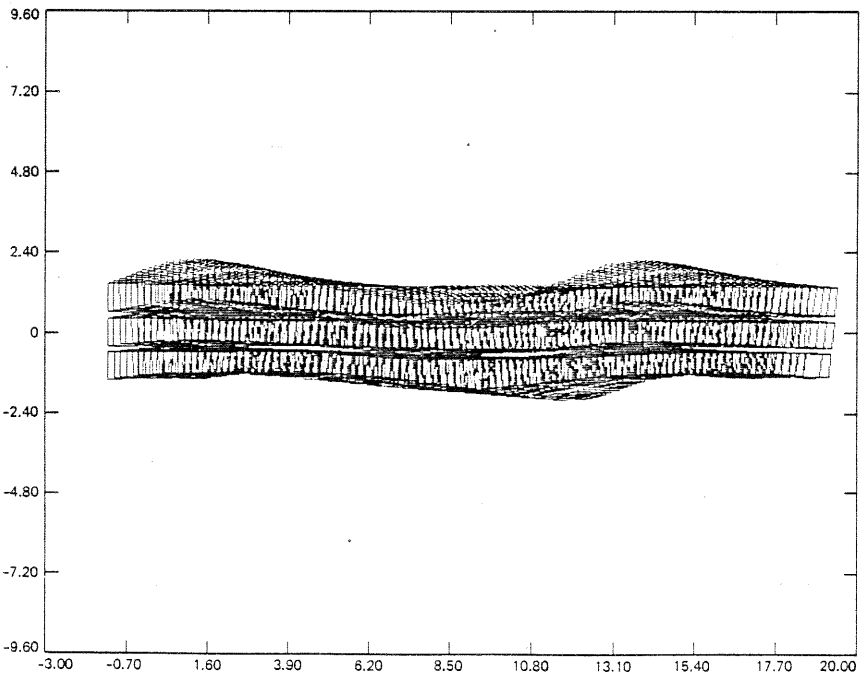


Figure 4. Ground path of the detector arrays.

In the small angle approximation trapezoidal projections of the square detector arrays can be accurately approximated by parallelograms, with the center, located at the intersection of the trapezoids diagonals. Extraction of the parallelogram subimage from the TM scene can then be done rather efficiently. The pixel values for equally spaced nodes of the parallelogram grid can be computed by the bi-linear interpolation of the four adjacent pixel values of the TM image. The time-sequence extracted in such a way is presented on Figure 5.

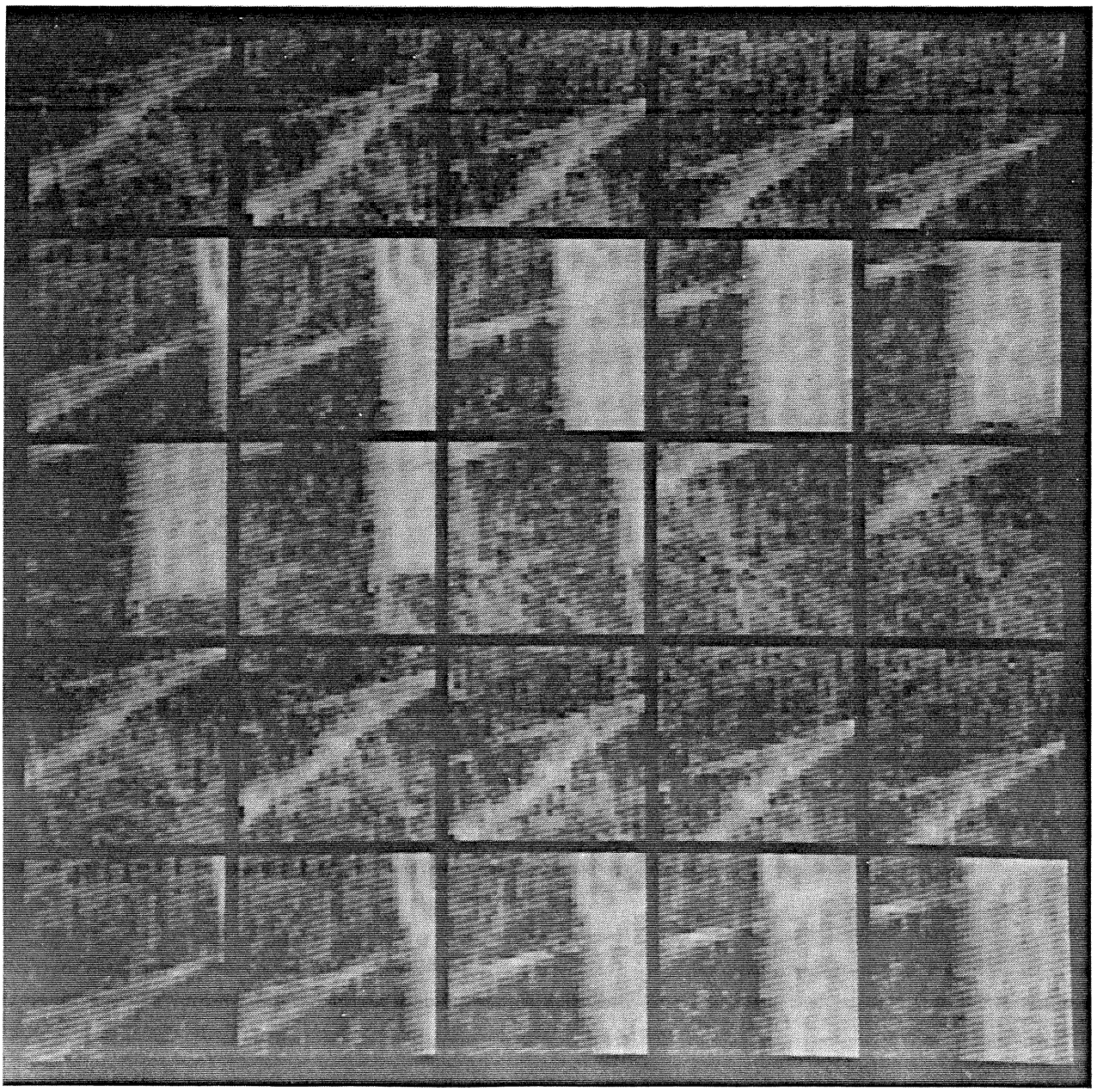

Figure 5. Time-sequence of images for detector #6.

## 4.2 Least-squares method validation

To test the approach described in section 3.3 we generated a sequence of lookpoint locations, varying roll, pitch and yaw from -0.1 to +0.1 radian, sinusoidally, with the period of 60 points and a phase shift of 0.79 and 1.57 radian. Then we resolved the equations 3.3.5 in the least-square sense. The results are shown on Figures 6 and 7. The deviation of the resolved angles from the original is very small everywhere, except near $\pm 0.1$ radian, when the linearization is no longer valid.

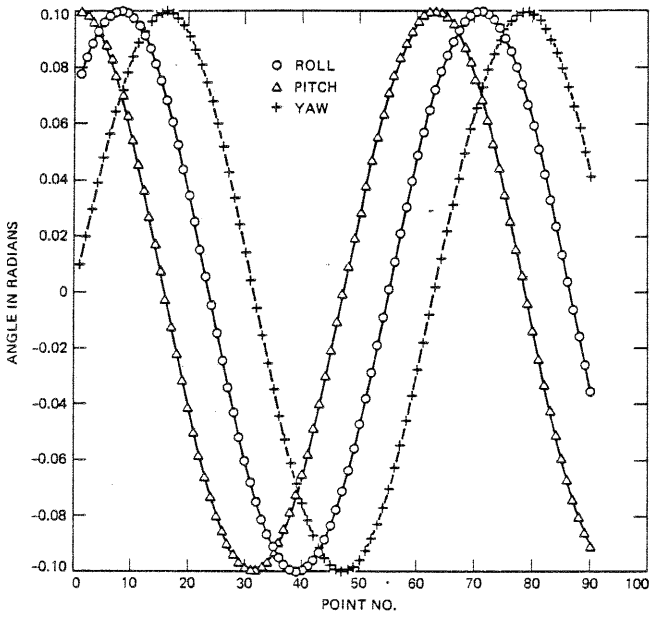


Figure 6. Original Euler angles.

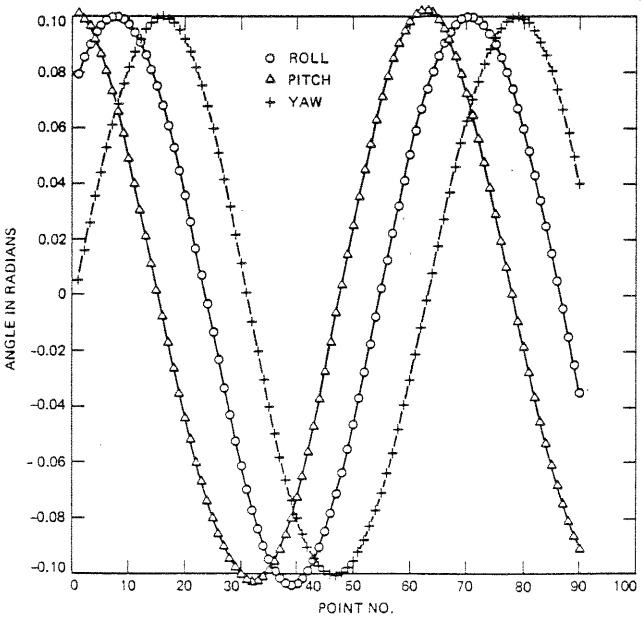


Figure 7. Recovered Euler angles, resolved by the least-squares fit, using displacements derived from the modelled angles.

## 4.3 Complete simulation

The results of a complete simulation are presented on Figure 8. We extracted the time-sequence of subimages for all nine detector arrays, by means of the two-dimensional FFT calculated the displacement vectors, and used those in the equations 3.3.5 to determine the attitude history.

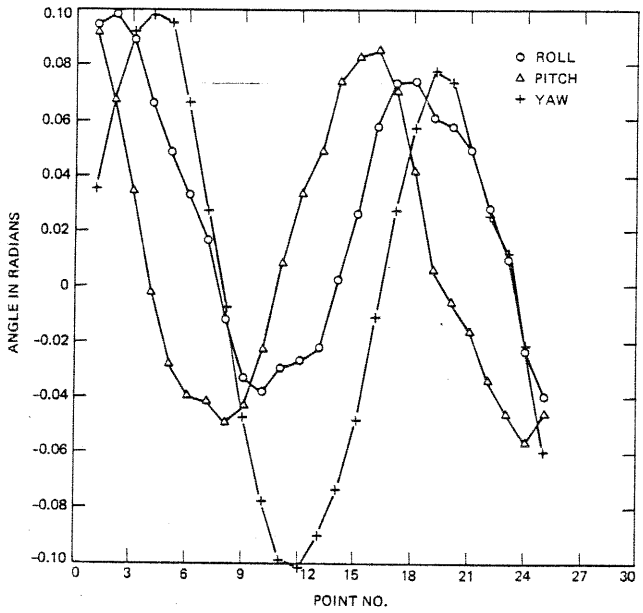


Figure 8. Simulation results, using displacements, derived fromm the FFT correlator.

One can immediately see that the extracted attitudes remain accurate only for a few initial iterations. The obvious and expected reason for errors is the accumulation and propagation of the measurement errors. In the equations (3.3.5) the ground position at every step is not a result of a direct measurement, but is calculated as a vector sum of a previous position and a displacement at this step.For n-th step we have:

$$\mathbf{r}'_n = \mathbf{r}'_{n-1} + \Delta \mathbf{r}_n$$

where $\Delta \mathbf{r}_n$ is measured by the FFT correlation.

For the correlator used, which determines the displacement to only the nearest pixel, the displacement vector accuracy is determined by the size of the resolution element of the detector array, and is equal to 1/2 the size of the pixel. It also depends on the frequency of correlations or, conversely, on the amount of overlap of the correlated subimages (i.e. the smaller the displacement, the larger relative error will be).

## 5. Conclusions and future work

We showed that it is possible to restore the attitude history of the platform by resolving the linearized system of motion equations and using the measured displacements of the small portions of the imaged scene.

The future research can progress in two directions:

1. System's design parameter simulation (size and spacing of the detector arrays, ratio of focal length to size, size and number of the resolution elements per array) to determine the optimal parameters for the eventual instrument, for both the satellite and the aircraft platforms.

2. Use of the Optimal Estimation methods (Kalman Filtering) to deal with the error accumulation problem.

## 6. Acknowledgements

We wish to acknowledge and thank the following for their assistance and counsel: Dr. Roy Welch, University of Georgia, Dr. Edward Mikhail and Dr. Fidel Paderes, Purdue University, Dr. Stephen Ungar and Dr. Samuel Gower, Goddard Space Flight Center, Dr. Nevin Bryant and Dr. Albert Zobrist, Jet Propulsion Laboratory.

This paper presents the results of one phase of research carried out at the Jet Propulsion Laboratory, California Institute of Technology, under contract to the National Aeronautics and Space Administration.

## 7. References

Billingsley, F. C., "Attitude Tracker", Proceedings of the NASA Workshop on Registration and Rectification, N. A. Bryant, Ed., JPL Publication 82-23, pp. 450-453, June 1982

Alspaugh, D. H., "Stereo Compilation and Digitizing", Proc. Latin American Technology Exchange Week, Panama City, May 1979, p. 314

Kuglin, C. D., Hines, D. C. "The Phase Correlator Image Alignement Method", Proc. IEEE 1975 International Conference on Cybernetics and Society, pp. 163-165.